Supporting Information

Structure-Activity Relationship of NF023 Derivatives Binding to XIAP-BIR1

Luca Sorrentino[+], Federica Cossu[+], Mario Milani, Bilge Malkoc, Wen-Chieh Huang, Shwu-Chen Tsay, Jih Ru Hwu,* and Eloise Mastrangelo*

Author Contributions

L.S. Conceptualization:Equal; Data curation:Lead; Methodology:Equal

Experimental Section

Infrared spectra (IR) were measured on a Fourier transform infrared spectrometer (FT-IR). Absorption intensities are recorded by the following abbreviations: s, strong; m, medium; and w, weak. Proton NMR spectra were obtained on a Varian Mercury-400 (400 MHz) or a Bruker AV-400 (400 MHz) spectrometer by use of dimethylsulfoxide-d_6 as the solvent. Carbon-13 NMR spectra were obtained on a Varian Mercury-400 (100 MHz) or a Bruker AV-400 (100 MHz) spectrometer. The residual solvent peaks, δ_H 2.50 ppm and δ_C 39.5 ppm for DMSO-d_6, were used as references. Multiplicities are recorded by the following abbreviations: s, singlet; d, doublet; t, triplet; q, quartet; m, multiplet; *J*, coupling constant (hertz). High-resolution mass spectra were obtained by means of a VARIAN-901 mass spectrometer.

Tatrasodium 4,4'-Carbonylbis(imino)bis-1,5-naphthalenedisulphonate (3).

mp (recrystallized from H_2O/EtOH) 193.6–194.2 °C; ^{1}H NMR (DMSO-d_6, 400 MHz) δ 8.80 (d, J = 8.0 Hz, 2 H, H-2), 8.05 (d, J = 8.0 Hz, H-3), 7.65 (d, J = 8.4 Hz, 2 H, ArH), 7.22 (t, J = 8.0 Hz, 2 H, H-7), 7.07 (s, 2 H, NH), 6.45 (d, J = 8.4 Hz, 2 H, ArH); ^{13}C NMR (DMSO-d_6, 100 MHz) δ 154.79 (C=O), 147.18, 143.20, 132.48, 130.52, 129.89, 126.44, 124.69, 122.92, 118.40, 107.36; IR (KBr) 3087 (w), 2989 (w), 1580 (s, C=O), 1423 (s), 1189 (m), 1042 (s), 835 (s) cm^{-1}; UV (Water): λ_{max} 253 (ε 11,804), 216 (ε 11,720), 342 (ε 5,171); HRMS (ESI) *m/z* [M + H]$^+$ calcd for $C_{21}H_{12}N_2Na_4O_{13}S_4$ + H 720.8891, found 720.8896.

Tatrasodium 4,4'-[Carbonylbis(imino-3,1-phenylenecarbonylimino)]bis-1,5-naphthalenedisulphonate (5a).

mp (recrystallized from H_2O/EtOH) 220.2–220.6 °C; ^{1}H NMR (DMSO-d_6, 400 MHz) δ 12.54 (s, 2 H, NH), 10.55 (s, 2 H, NH), 9.10 (d, J = 8.8 Hz, 2 H, ArH), 8.29 (d, J = 8.8 Hz, 2 H, ArH), 8.07–8.01 (m, 6 H, ArH), 7.83–7.79 (m, 4 H, ArH), 7.45 (t, J = 8.8 Hz, 2 H, ArH), 7.35 (t, J = 8.0 Hz, 2 H, ArH); ^{13}C NMR (DMSO-d_6, 100 MHz) δ 165.70 (C=O), 153.17 (C=O), 141.71, 140.98, 140.28, 136.21, 134.53, 131.57, 130.70, 128.21, 127.04, 124.57, 123.48, 123.45, 122.39, 120.88, 120.68, 118.11; IR (KBr) 3355 (br, NH), 2919 (m), 1652 (m, C=O), 1575 (s), 1545 (s), 1524 (s), 1193 (s), 1044 (s), cm^{-1}; UV (Water): λ_{max} 234 (ε 11,641), 311 (ε 6,872); HRMS (ESI) *m/z* [M + Na]$^+$ calcd for $C_{35}H_{22}N_4Na_4O_{15}S_4$ + Na 980.9447, found 980.9446.

Tatrasodium 4,4'-(Carbonylbis[imino-3,1-(4-methylphenylene)carbonylimino])bis-1,5-naphthalenedisulphonate (5b).

mp (recrystallized from H_2O/EtOH) 224.4–224.8 °C; ^{1}H NMR (DMSO-d_6, 400 MHz) δ 12.50 (s, 2 H, NH), 9.09 (s, 2 H, NH), 9.06 (d, J = 7.6 Hz, 2 H, ArH), 8.35 (s, 2 H, H-2'), 8.28 (d, J = 8.0 Hz, 2 H, ArH), 8.02−8.00 (m, 4 H, ArH), 7.84 (d, J = 7.6 Hz, 2 H, ArH), 7.45 (t, J = 8.0 Hz, 2 H, H-7), 7.26 (d, J = 8.0 Hz, 2 H, ArH), 2.39 (s, 6 H, 2 × CH_3); ^{13}C NMR (DMSO-d_6, 100 MHz) δ 165.61 (C=O), 153.32 (C=O), 141.77, 140.82, 137.51, 134.66, 133.74, 132.18, 131.58, 130.69, 129.68, 127.01, 126.90, 124.61, 123.47, 123.42, 122.37, 122.29, 18.48 (CH_3); IR (KBr) 3354 (br, NH), 3048 (w), 2914 (s), 2848 (m), 1635 (s, C=O), 1575 (m), 1424 (m), 1225 (w) cm^{-1}; UV (Water): λ_{max} 236 (ε 15,050), 310 (ε 10,288); HRMS (ESI) *m/z* [M + Na]$^+$ calcd for $C_{37}H_{26}N_4Na_4O_{15}S_4$ + Na 1008.9760, found 1008.9765.

Disodium 4-(3-[3-(Ethoxylthioxoimino)benzamido]-4-tolylamido)naphthalene-1,5-disulphonate (9).

mp (recrystallized from H_2O/EtOH) 205.4–205.6 °C; ^{1}H NMR (DMSO-d_6, 400 MHz) δ 8.89 (d, 1 H, J = 8.8 Hz, ArH), 8.31 (d, J = 8.8 Hz, 1 H, ArH), 7.63 (d, J = 7.6 Hz, 1 H, ArH), 7.44 (s, 1 H, ArH), 7.39 (s, 1 H, ArH), 7.30–7.26 (m, 2 H, ArH), 6.88 (t, J = 7.6 Hz, 1 H, ArH), 6.67 (d, J = 7.6 Hz, 1 H, ArH), 6.60–6.43 (m, 3 H, ArH), 4.11 (q, J = 6.8 Hz, 2 H, OCH_2), 2.05 (s, 3 H, CH_3), 1.03 (t, J = 6.8 Hz, 3 H, CH_3); ^{13}C NMR (DMSO-d_6, 100 MHz) δ 183.55 (C=S), 165.65 (C=O), 165.15 (C=O), 147.03, 144.58, 139.99, 136.26, 135.29, 133.62, 131.96, 130.28, 128.98, 127.89, 126.99, 125.64, 125.39, 123.26, 122.78, 122.71, 122.71, 120.10, 118.31, 116.72, 114.62, 113.36, 66.03, 18.53, 14.51; IR (KBr) 3346 (br, NH), 2927 (s), 1646 (s, C=O), 1574 (w), 1544 (m), 1422 (m), 1334 (m), 1227 (m) cm^{-1}; HRMS (ESI) *m/z* [M + H]$^+$ calcd for $C_{28}H_{23}N_3Na_2O_9S_3$ + H 688.0470, found 688.0478.

^{1}H-NMR, ^{13}C-NMR, and IR Spectra as well as HRMS Data of Sodium Organosulfonates 3, 5a, 5b, and 9

Compound 3

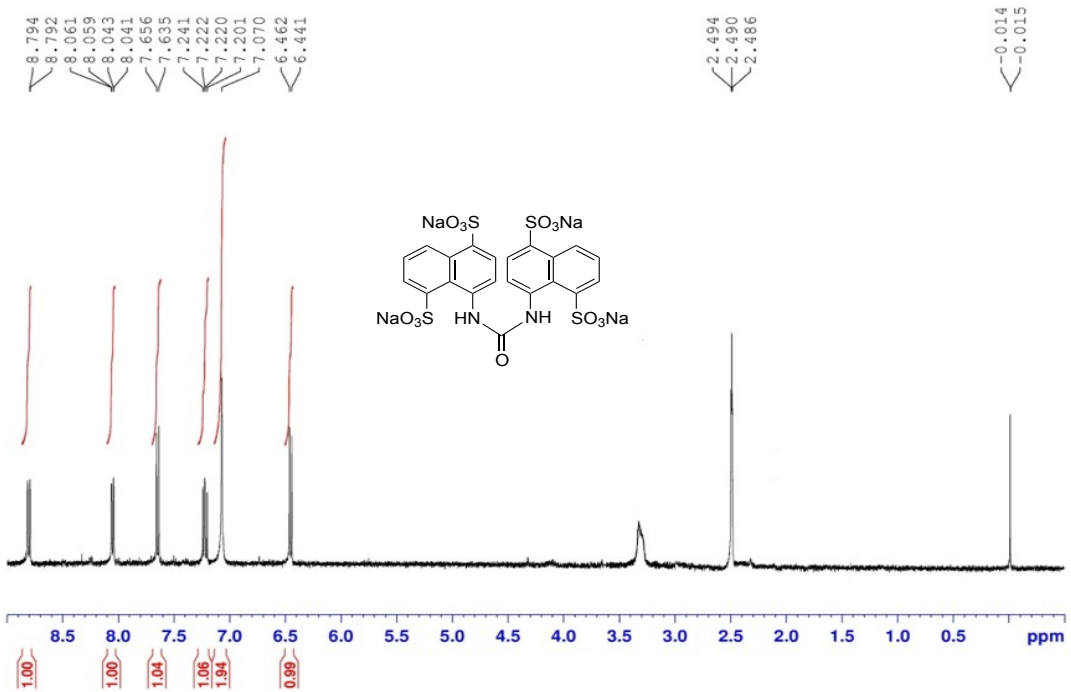

^{1}H NMR spectrum of salt **3**

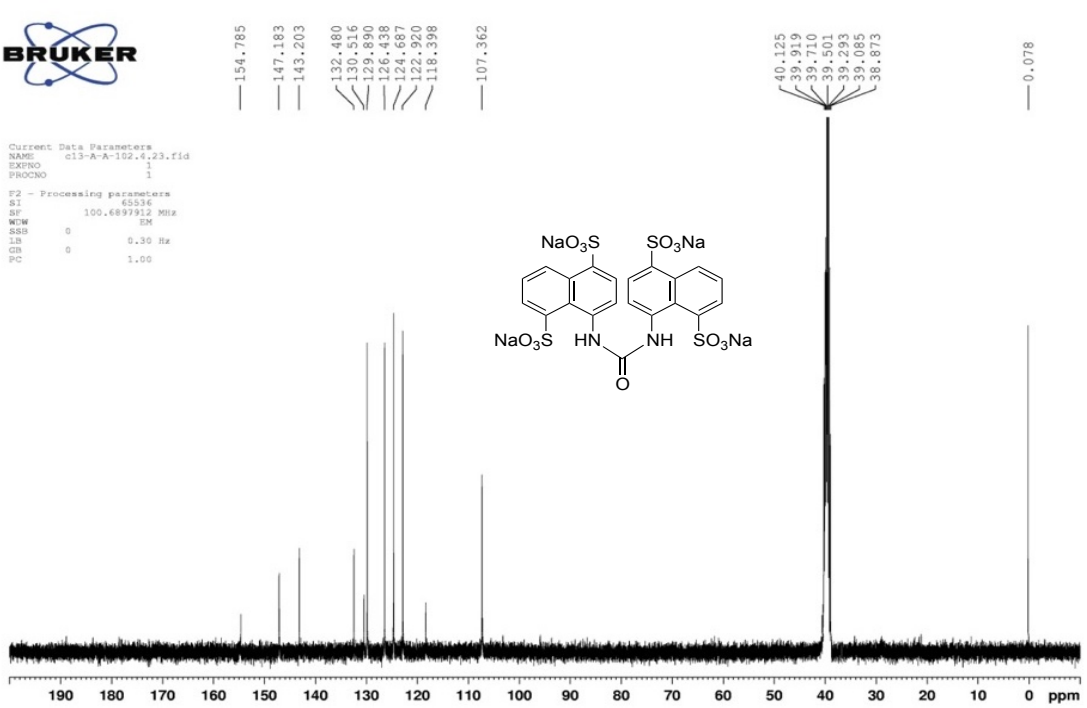

^{13}C NMR spectrum of salt **3**

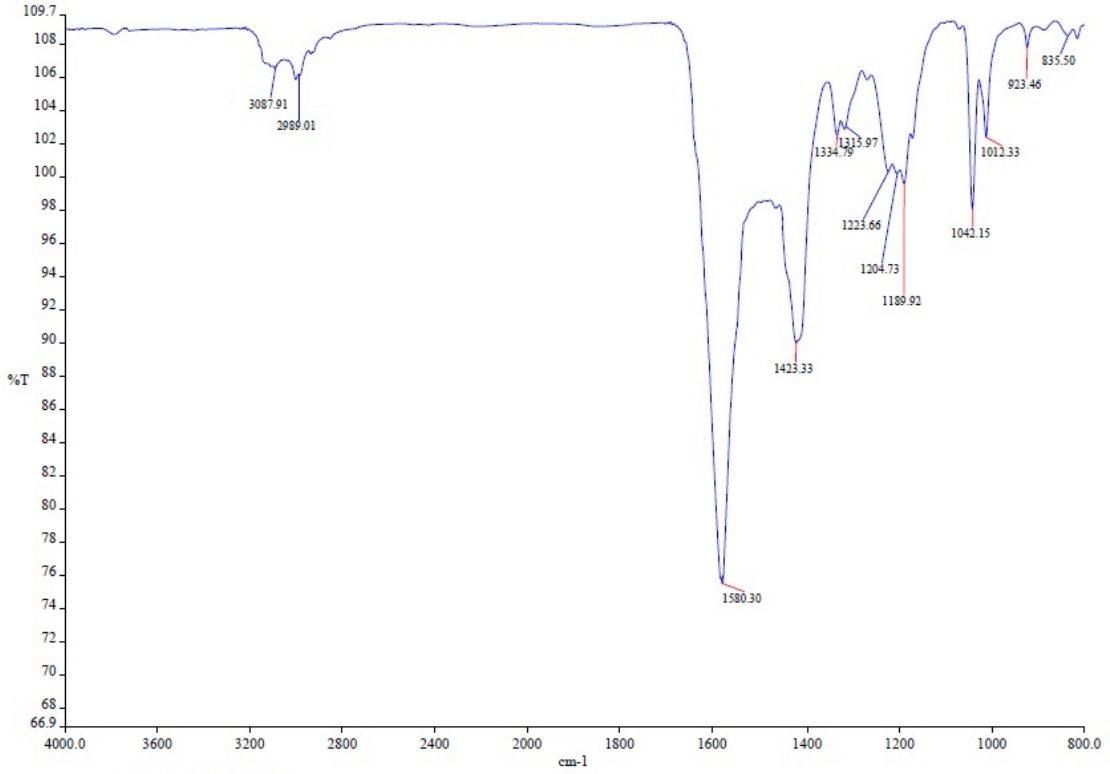

IR Spectrum of salt **3**

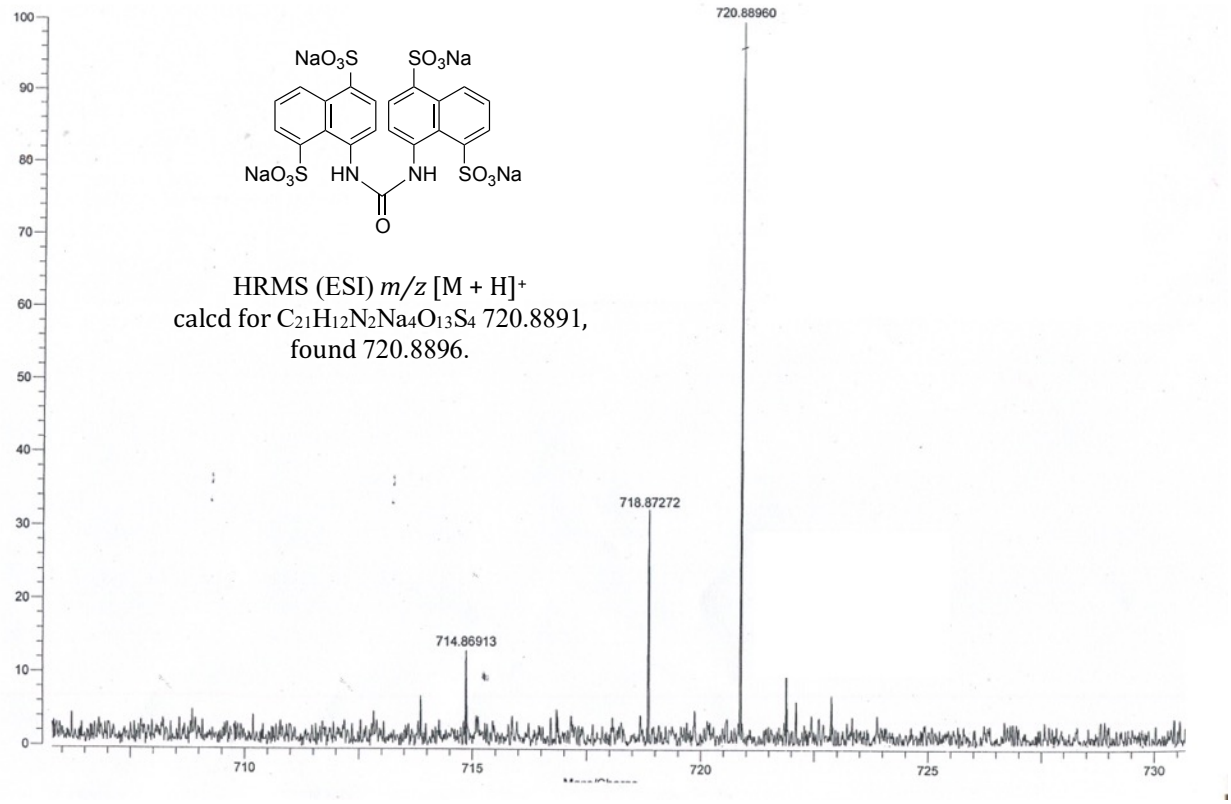

HRMS (ESI) m/z $[M + H]^+$
calcd for $C_{21}H_{12}N_2Na_4O_{13}S_4$ 720.8891,
found 720.8896.

HRMS of salt **3**

Compound 5a

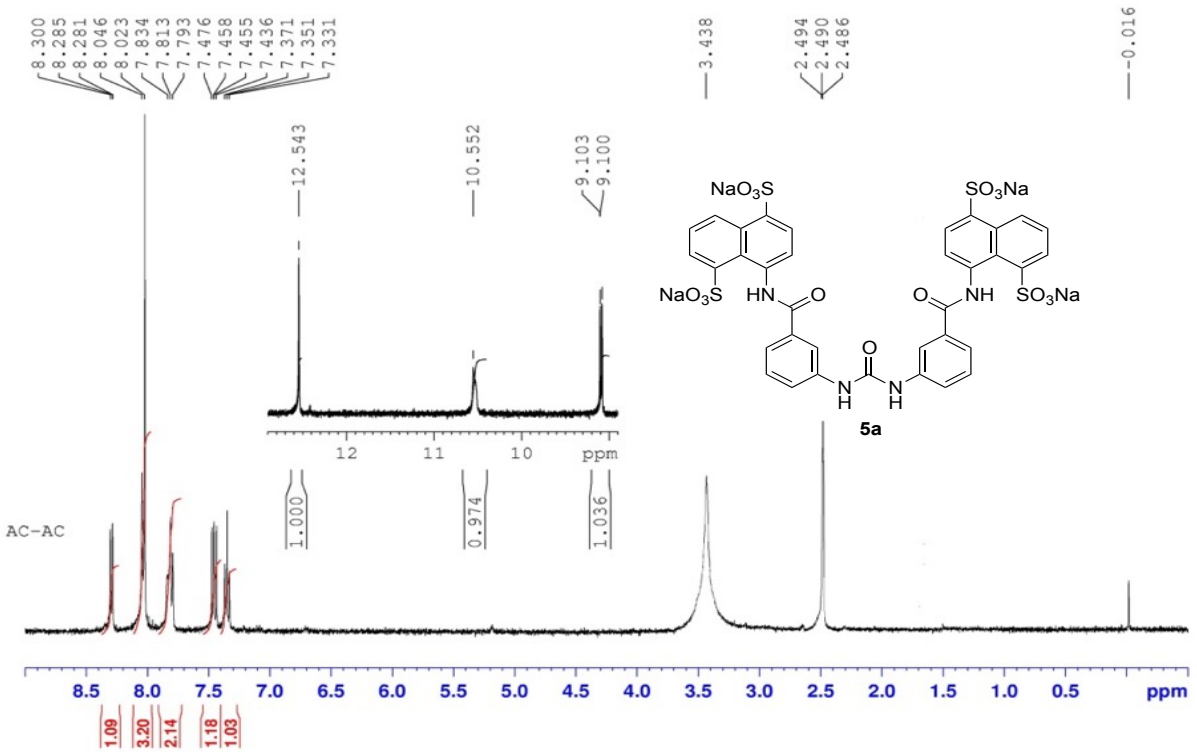

^{1}H NMR spectrum of salt **5a**

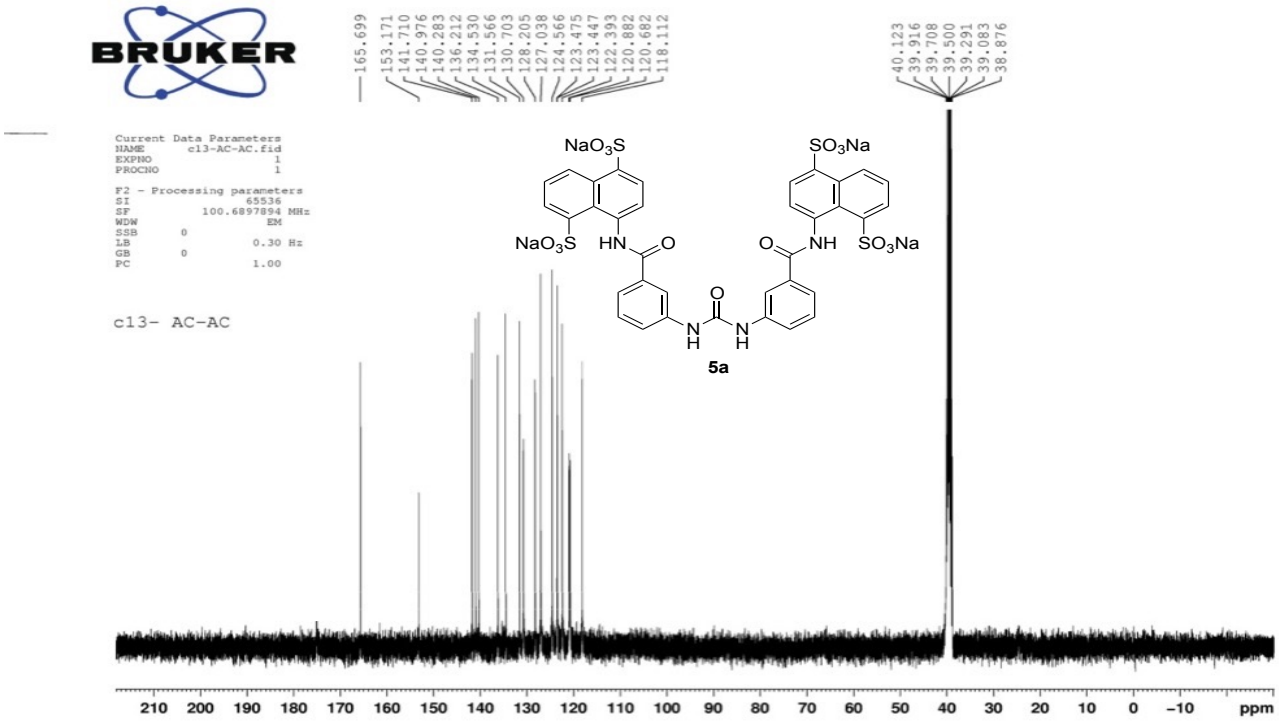

^{13}C NMR spectrum of salt **5a**

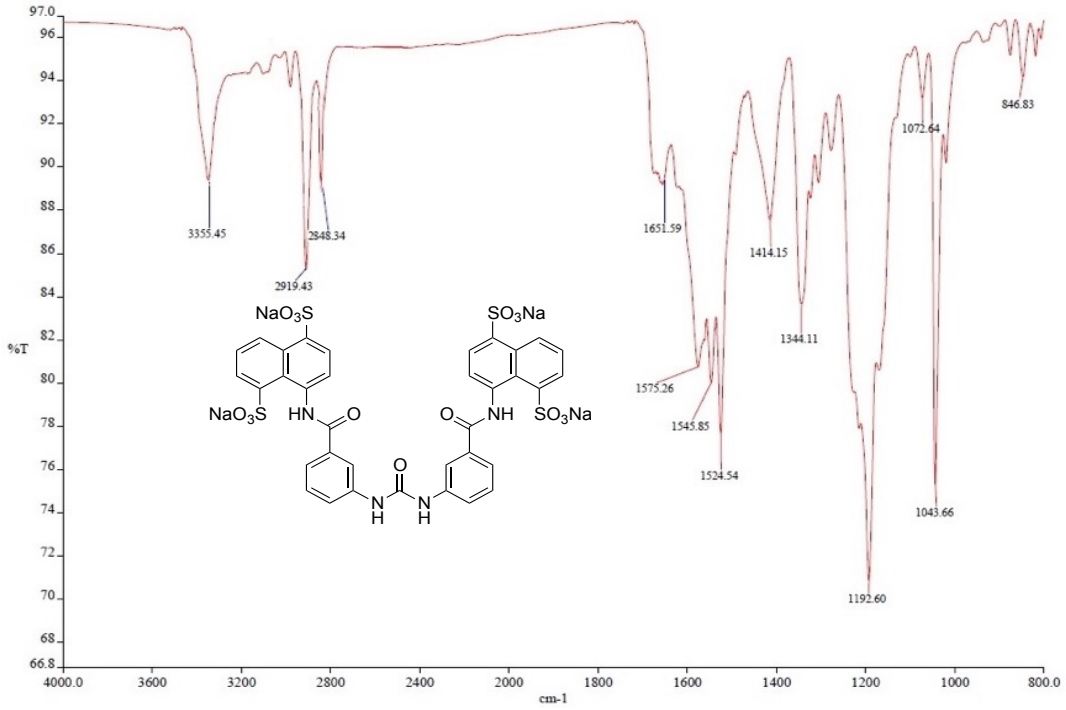

IR Spectrum of salt **5a**

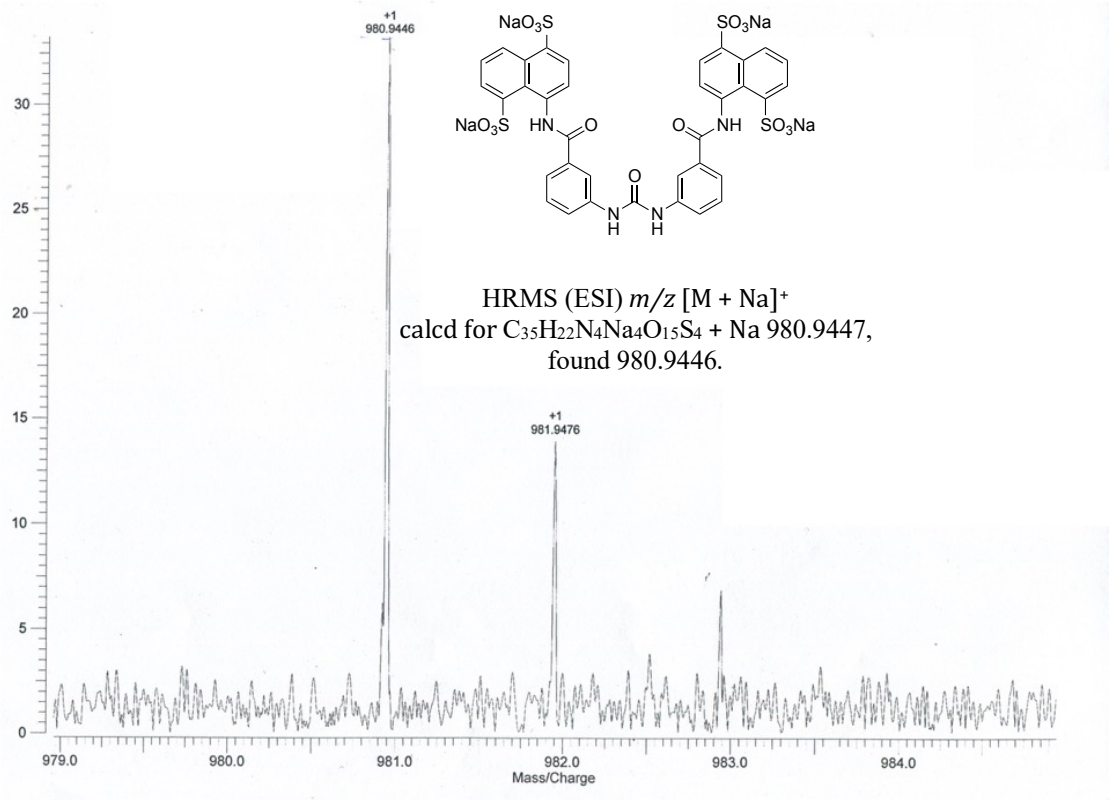

HRMS (ESI) m/z $[M + Na]^+$
calcd for $C_{35}H_{22}N_4Na_4O_{15}S_4$ + Na 980.9447,
found 980.9446.

HRMS of salt **5a**

Compound 5b

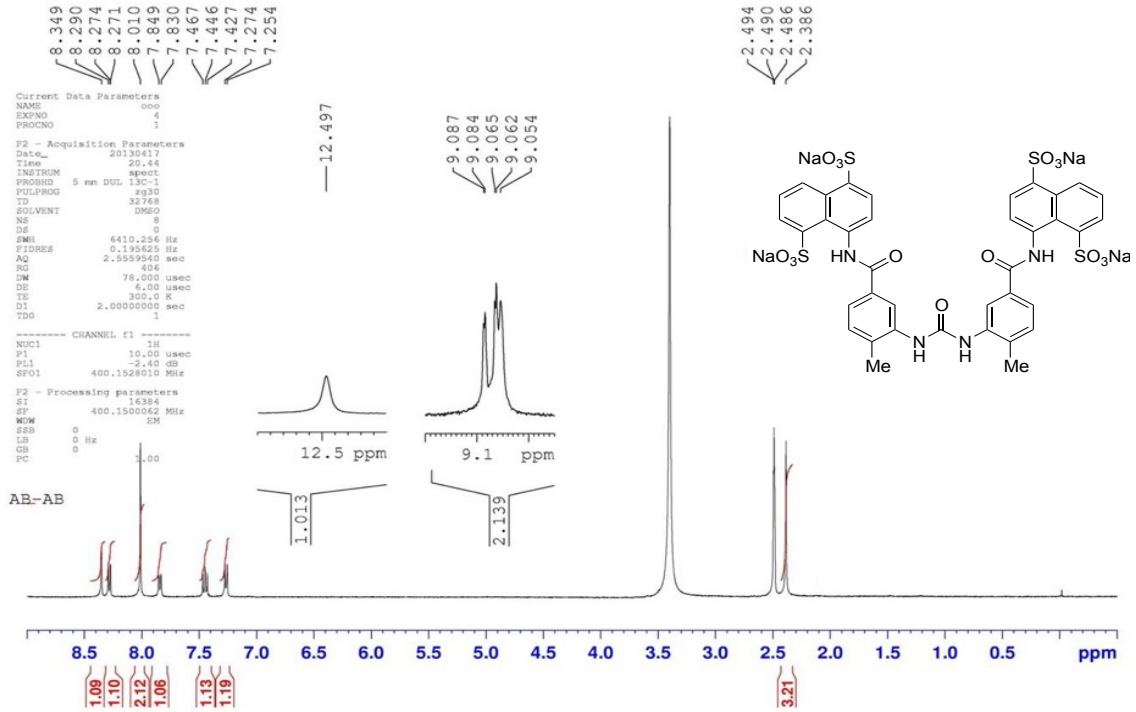

^{1}H NMR spectrum of salt **5b**

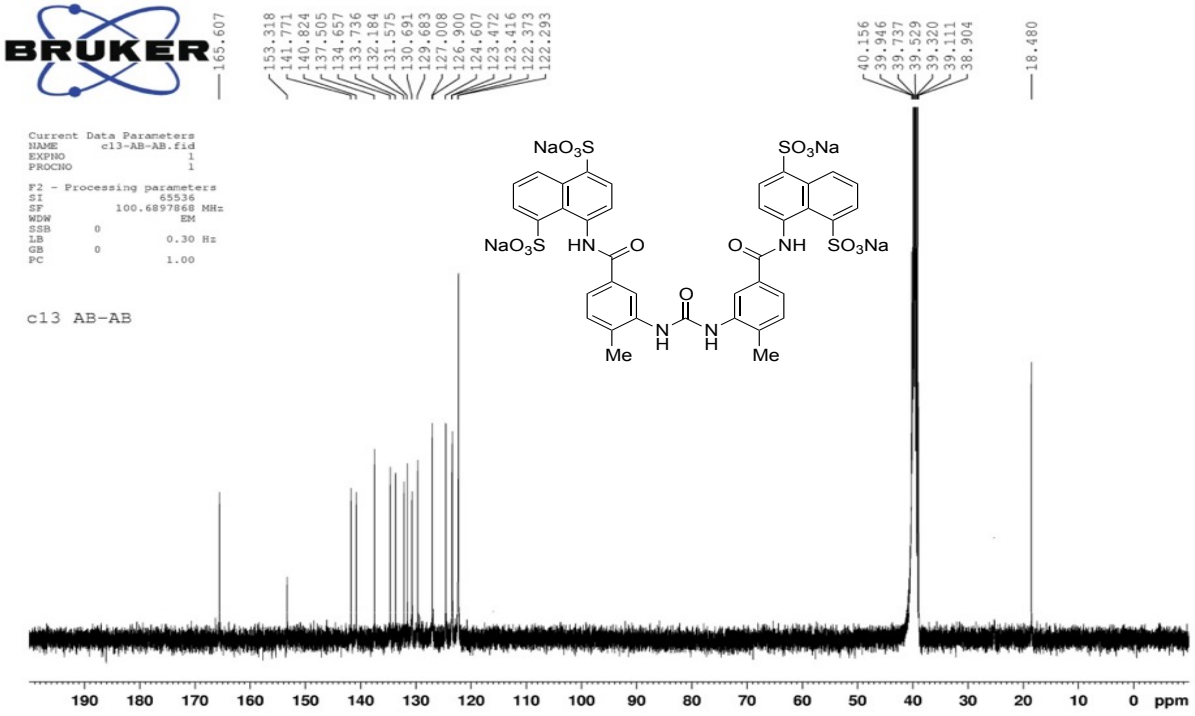

^{13}C NMR spectrum of salt **5b**

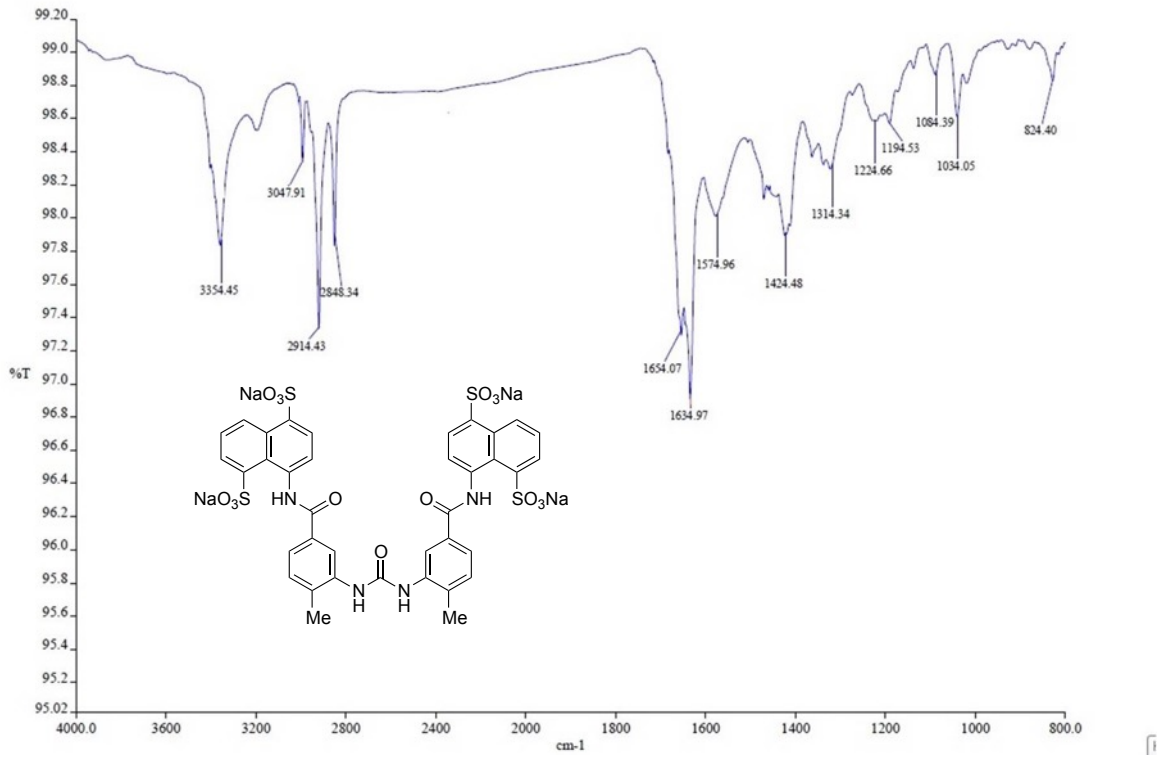

IR Spectrum of salt **5b**

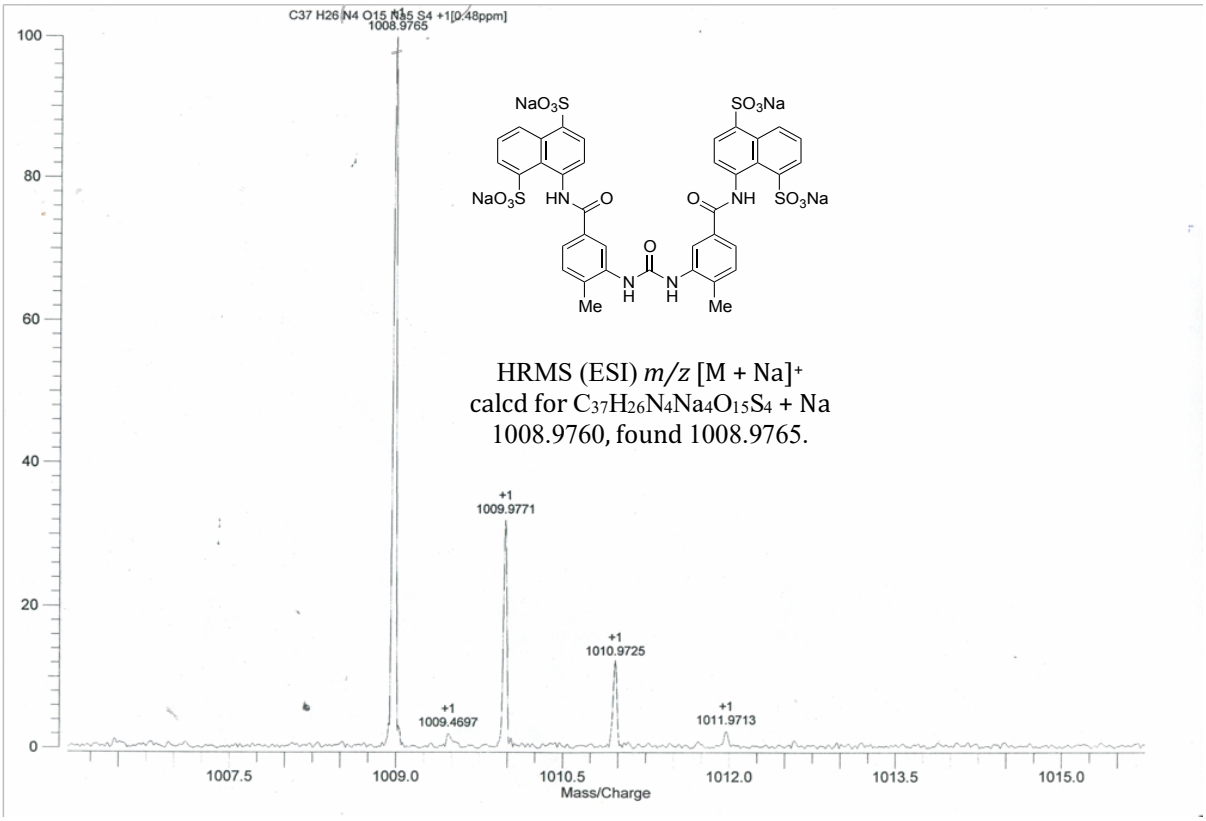

HRMS (ESI) *m/z* $[M + Na]^+$
calcd for $C_{37}H_{26}N_4Na_4O_{15}S_4$ + Na
1008.9760, found 1008.9765.

HRMS of salt **5b**

Compound 9

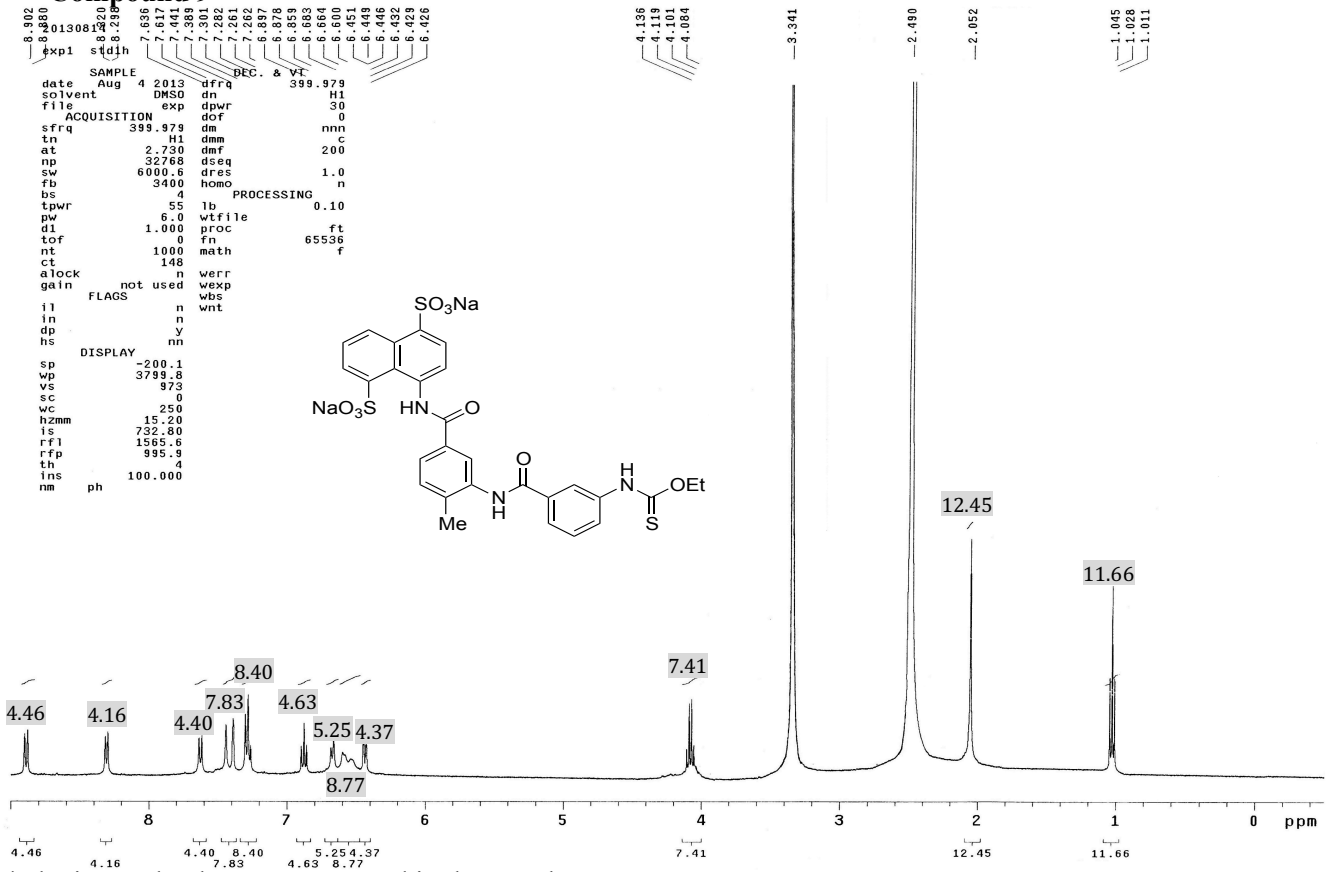

*The integral values are presented in the gray boxes.

^{1}H NMR spectrum of salt **9**

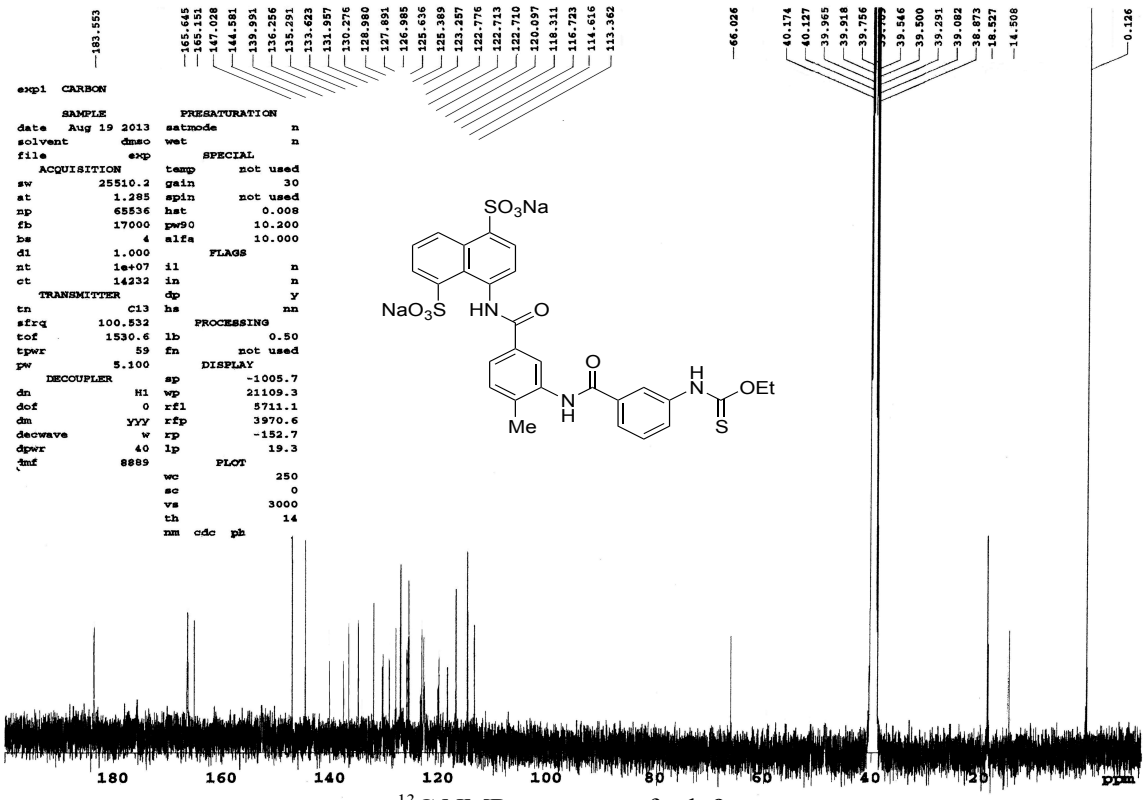

^{13}C NMR spectrum of salt **9**

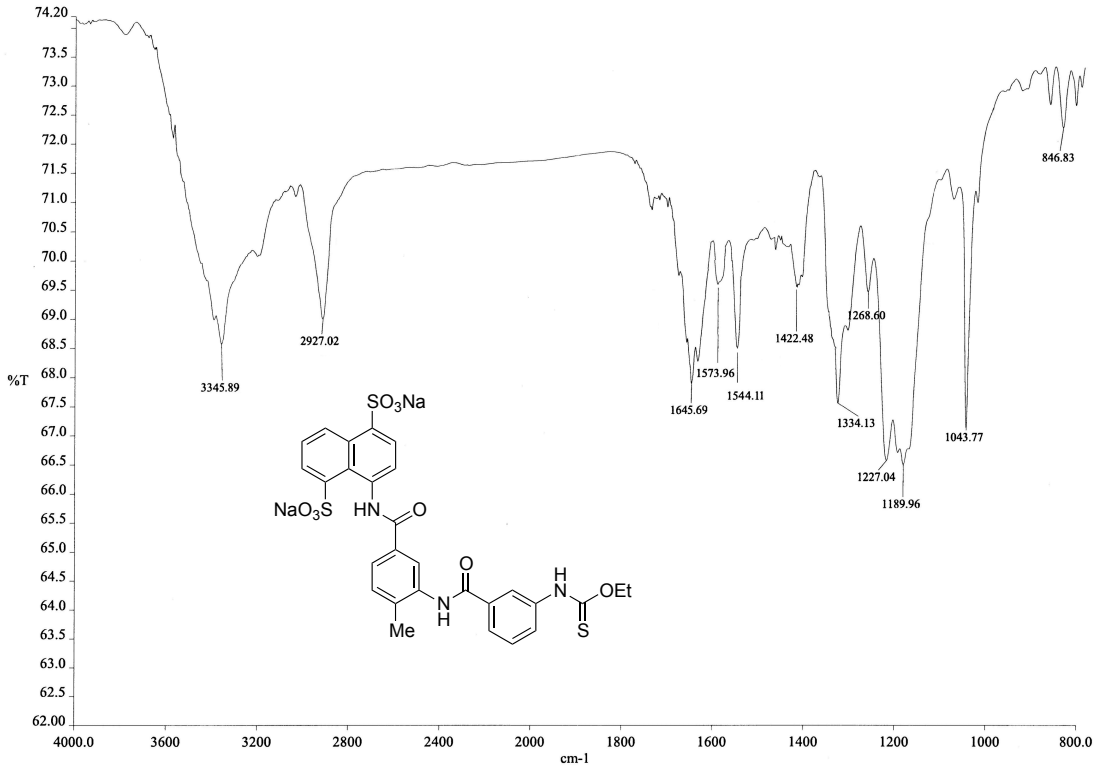

IR spectrum of salt **9**

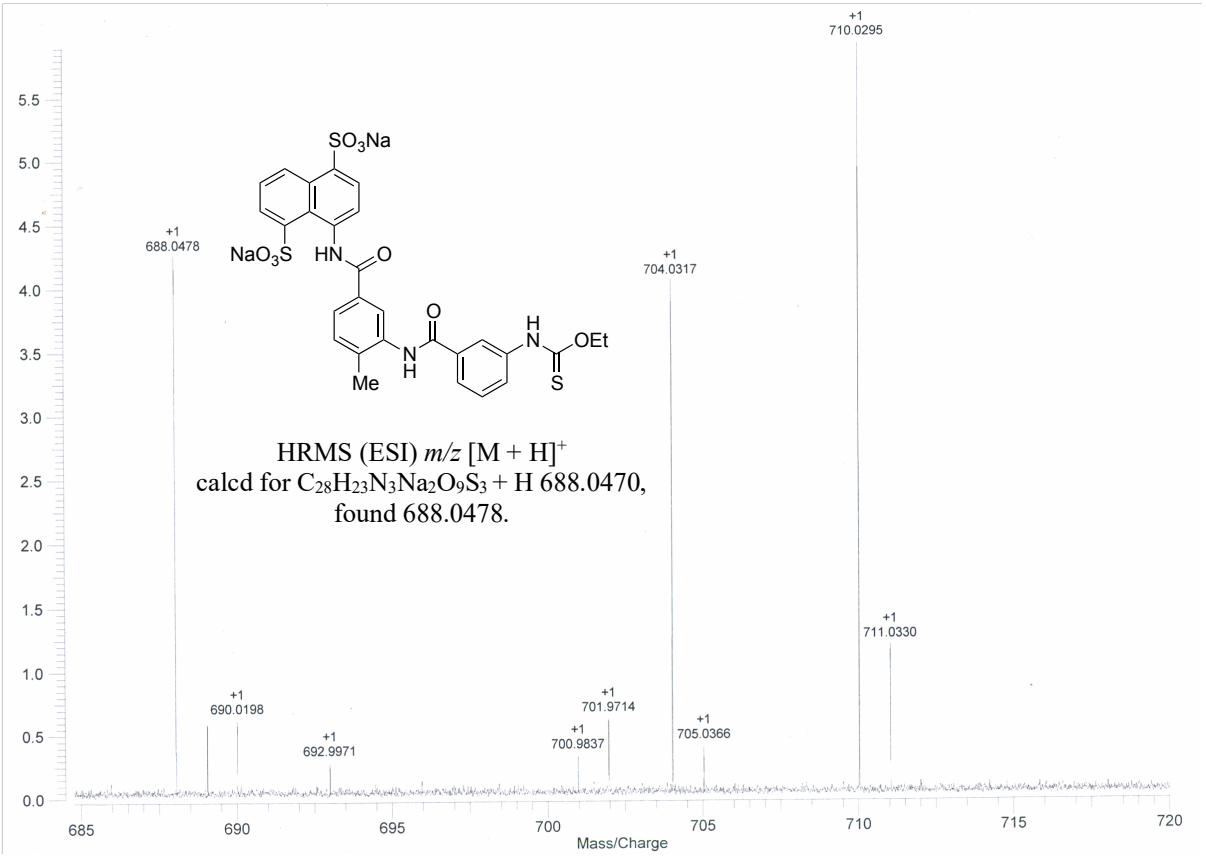

HRMS (ESI) *m/z* $[M + H]^+$
calcd for $C_{28}H_{23}N_3Na_2O_9S_3$ + H 688.0470,
found 688.0478.

HRMS of salt **9**

Table S1. XIAP-BIR1 thermal stability and affinity for NF023 like molecules moieties.

Sample	Compounds Chemical Structure	Melting Temperature (°C)	ΔT_m (°C)[a]
XIAP-BIR1	/	63.5 ± 0.9	/
XIAP-BIR1/NF023	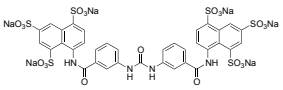	56.7 ± 1.0	–6.8
XIAP-BIR1/Suramin	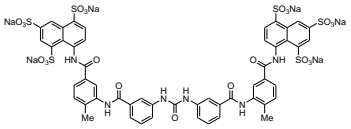	50.0 ± 0.5	–13.5
XIAP-BIR1/**3**	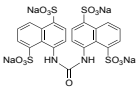	63.0 ± 0.3	–0.5
XIAP-BIR1/**5a**	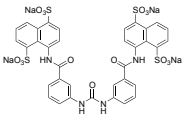	56.2 ± 0.3	–7.3
XIAP-BIR1/**5b**	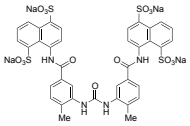	56.2 ± 0.3	–7.3
XIAP-BIR1/**6**	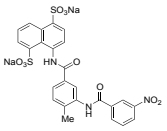	60.5 ± 0.1	–3.0
XIAP-BIR1/**7**	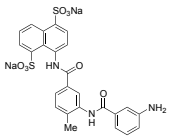	60.5 ± 0.2	–3.0
XIAP-BIR1/**9**	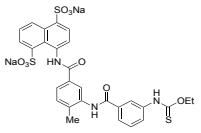	62.5 ± 1.5	–1.0
XIAP-BIR1/**10**	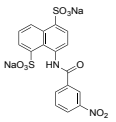	61.2 ± 0.6	–2.3
XIAP-BIR1/NAF2		61.0 ± 0.3	–2.5

[a]ΔT_m is calculated as the difference from the apoprotein melting temperature.

Thermal shift assays to monitor unfolding of 80 μM XIAP-BIR1 (~1 mg/ml) upon incubation with 1.0 mM of each compound were conducted in a MiniOpticon Real-Time PCR Detection System (Bio-Rad). The fluorescent dye Sypro Orange was used to monitor protein unfolding. The sample plates were heated from 15 to 95 °C, with a heating rate of 0.5 °C/5 sec. Fluorescence intensity was measured within the excitation/emission ranges 470–505/540–700 nm. All the experiments were performed in triplicate, to calculate average T_M values and associated standard errors.

Suramin (ΔT_m of about –13.5°C), NF023 and its analogs **5a** and **5b** (ΔT_m of about –7°C), and compounds **6** and **7** (ΔT_m of about –3°C) caused a significant effect on the protein conformational stability.

Figure S1. The V86E mutation is compatible with NF023 predicted binding. The structure of XIAP-BIR1 V86E mutant (in magenta) superimposed to XIAP-BIR1/NF023 docking prediction (light blue cartoons and green sticks) reveals that the steric hindrance of E86 side chain is fairly compatible with NF023 predicted binding, as confirmed by MST experiments, where the measured affinity of NF023 *vs* XIAP-BIR1 V86E is not drastically affected compared to the value observed *vs* the wild type protein domain.